

大韓造船學會論文集
 제 30 卷 第 3 號 1993年 8月
 Transactions of the Society of
 Naval Architects of Korea
 Vol. 30, No. 3, August 1993

Vortex Cloud Model에 의한 주상체 주위의 Vortex 유출 Simulation

이동기*

Simulation of the Vortex Shedding from a Circular
 Cylinder by Means of the Vortex Cloud Model

by

D.K. Lee*

요 약

균일한 정상유동을 하는 유체 안에 가로놓인 원주로부터 일어나는 vortex 유출을 이산 vortex 방법을 써서 vortex cloud 모형으로 simulation 했다. 원주표면에서 생겨나는 와도를 매 시간 간격마다 미리 정해진 많은 갯수의 이산화된 초생 vortex로 나타낸 후 기 유출된 vortex들에 합류시켜 누적된 vortex들의 운동을 탐색함으로써 vortex 분포 상태의 진화를 알아낸다. vortex들의 이동은 cloud-in-cell 기법을 써서 추적 하였고 항력 계수와 양력 계수는 Sarpkaya의 식과 Lee의 식을 써서 계산하여 실험치와 비교하였다. 계산 인수 사이의 상호 연관 관계를 논고하였으며 부분적이거나 적정값 선정 원칙을 제시하였다.

Abstract

The vortex shedding from a circular cylinder placed in a steady uniform stream is simulated by the vortex cloud model of the discrete vortex method. The vorticity created at the cylinder surface is discretely represented by a number of nascent vortices at each time step and the motion of these cumulative vortices is monitored to produce the evolution of the vortex distribution pattern. Convection of vortices was traced by the vortex-in-cell technique and the force coefficients were calculated by both Sarpkaya's formulae and Lee's formulae for comparison. Discussions concerning the interrelation between the computational parameters and some principles for choosing the suitable values are included.

접수일자 : 1993년 1월 28일, 재접수일자 : 1993년 3월 22일

* 정회원, 울산대학교 조선공학과

This paper was supported by NON DIRECTED RESEARCH FUND,
 Korea Research Foundation, 1991

1. Introduction

The flow around a circular cylinder can be analysed by a number of different methods of attacking the equation of motion. As one of these, the discrete vortex method (referred to the DVM in the following) has in recent years attracted much attention by producing some impressive results for shed vortex distribution patterns which are claimed to assume high Reynolds number flows. When vorticity is the major matter of interest, this method is a preferable choice to other ways of dealing with the flow fields since it makes use of and appreciates the intrinsic properties of vortex dynamics in tracing the flow evolution. It may be noteworthy that the method is particularly suitable for two-dimensional problems owing to the characteristic nature of vortex lines. Also the fact that the results produced by the DVM are not blown up directly with increasing Reynolds number has some significance in numerical treatments of flow fields.

The first attempt to represent the shear layers emanating from a blunt body by discrete vortices was made by Gerrard[1]. His sheet vortex model of vortex shedding was further exploited and refined by Clements[2], Sarpkaya[3] and others, and Fink and Soh[4] developed the effective technique of discretising the sheet vortex to postpone onset of the numerical instability as late as possible. However it was not so long before the shortcomings of this model for representing what is happening in the boundary layer and the wake are felt acutely. The vortex cloud model[5] appeared to meet what is wanted. A number of vortices are put around the cylinder on a certain principle at every sequential time step and the evolution of the pattern composed by their subsequent instantaneous positions is traced in this model. No specific strategy is necessary to find the separation points as they are determined in the course of shedding of these vortices. The diffusion of vorticity by the viscous effect can be taken to some degree into consideration by

incorporating the so-called random walk method to the calculation, which will no doubt bring some difference in the flow field for flow of different Reynolds number.

However it is too early to say that the Reynolds number dependency of a flow can be adequately accounted for by this model because the random walk technique is only an ad-hoc improvisation to simulate the diffusion process rather than a built-in structure of the method. There are still quite a few methodical snags to be resolved before this fundamental, yet difficult to meet, requirement can ever be thought seriously. Diffusion of vorticity is therefore excluded in the present study resulting in a flow model of the inviscid fluid with strength-preserving imbedded vortices. Removal of the arbitrary computational parameters is one of the related tasks to which attention of the present paper is directed. These parameters do not play independent roles but have some interrelationship between them which will be one of the important topics of discussion. Even if the interrelationship is fully disclosed and the arbitrariness is reduced to the minimum, there should remain truly arbitrary factors in this model. The remedy for stimulating asymmetry of flow is one of those, about which a brief, though important, guideline is mentioned. When the fundamental unavoidable factors of arbitrary magnitude and the strategy to stimulate the asymmetry are fixed, the set of computational parameters, to be found only through numerical experiments, that will bring forth the best pattern of vortex distribution is a matter of keen interest since it has general meanings due to the use of nondimensional variables. A set which seems to work well is presented.

The force exerted to the cylinder by fluid is of course the most important end product of the computational scheme. It has usually been calculated with the Sarpkaya's formulae[6]. Lee[7] suggested the modified formulae which contain terms concerned with the growth rate of the strength of the nascent vortices. The force is

calculated by the both sets of formulae for comparison.

2. Representation of the flow field

A circular cylinder of radius a is placed within a uniform flow of magnitude U directed toward the positive x -direction. The origin of the coordinate system is chosen at the center of the cylinder. All the variables except those mentioned otherwise are supposed to be nondimensionalized with respect to U and a . The plane outside the cylinder is covered by grid composed of m equally-spaced radial lines and n concentric circular arcs specified by the following equations :

angle between the radial lines :

$$\Delta\theta = 2\pi/m \quad (2.1)$$

radius of the k -th circular arc :

$$r_k = r_1(1 + \Delta\theta)^{k-1}, \quad k = 1, 2, \dots, n \quad (2.2)$$

$$\text{with } r_1 = 1 + \epsilon \quad (2.3)$$

A cell generated by this pair of equations is fan-shaped with the equal radial and inner circumferential lengths. The parameter m determines the degree of resolution of the flow field.

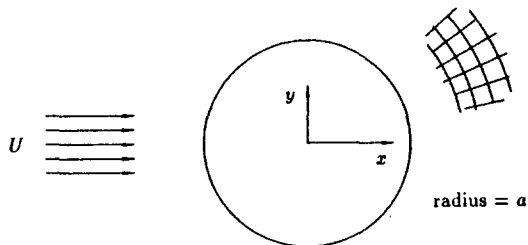


Fig. 1 The flow field

A positive number ϵ to be much smaller than δ the distance between a nascent vortex and the cylinder surface is needed to prevent the innermost nodes from coinciding with the cylinder sur-

face. Without this, when the shed vortex strengths are allotted to the nodes, the nodal vortex strengths on the innermost nodes are nullified as they coincide with their images, creating a large error for the motion of the vortices lying within the first layer of the grid. The value used for it in the present study is 0.01.

2.1 The boundary condition

The condition of zero normal component of velocity is usually dealt with by the use of image vortex concept in the DVM as is the case in the present study. The image vortex system within the circular cylinder for an external vortex is simple due to the simplicity of the body geometry and is composed of just one vortex of the same strength but opposite sign at the inverse point. This image vortex system is different from that specified by the Milne-Thomson's circle theorem [8], in that no vortex is put at the cylinder center. It is thought to be appropriate for modelling vorticity creation at the cylinder surface with the DVM approach because there should be no net circulation on a closed circular contour of radius large enough to enclose the cylinder and the external vortex. The complex potential of a vortex located at any point external to the cylinder is then

$$\varphi(z) = -\frac{i}{2\pi}\Gamma \left[\log(z - z_o) - \log(z - z_i) \right] \quad (2.4)$$

where z_i : the inverse point of

$$z_o, z_i = 1 / \bar{z}_o \quad (2.5)$$

z_o : position of the vortex

Γ : strength of the vortex.

The no slip condition is satisfied, in the most DVM analysis of flow about a cylindrical body, by determining the strengths of the nascent vortices so that the condition is realized at every control point on the cylinder surface. This principle, in spite of its logical clearness and sim-

plicity, has a serious drawback that the strengths of vortices so determined are strongly dependent on the distance between the chosen positions of the nascent vortices and the cylinder surface and no uncontroversial guideline for the choice of suitable distance is devised so far. This consideration suggested an indirect way of satisfying the condition by determining strength of a nascent vortex as the local tangential velocity at the corresponding control point on the cylinder surface multiplied by the circumferential segment length.

2.2 The vortex-in-cell[9] technique

2.2.1 The nodal distribution of vortices

All the vortices shed in the flow field are distributed to nodes of the grid at every time step. The bivariate linear redistribution scheme is usually employed for this purpose and the result is :

$$\Gamma_i = \Gamma \frac{A_i}{A}, \quad i = 1, \dots, 4 \quad (2.6)$$

where A ; area of the cell

A_i : the partitioned area element opposite to the i -th corner, see Fig. 2

This equation is applied in turn to every vortex

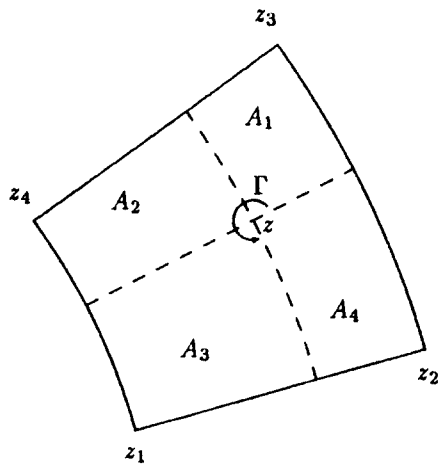


Fig. 2 Area division of a cell

existing in the flow field at a particular time step to produce the regular nodal distribution of vortices which replaces the original spontaneous one. This regular nodal distribution is used only for the calculation of velocities at the nodes.

A_i 's in eq. (2.6) are calculated from

$$\begin{aligned} A_1 &= \frac{1}{2} |\Im(\bar{z} z_3)| \left(\frac{1}{r_o} + \frac{1}{r} \right) (r_o - r) \\ A_2 &= \frac{1}{2} |\Im(\bar{z} z_4)| \left(\frac{1}{r_i} + \frac{1}{r} \right) (r - r_i) \\ A_3 &= \frac{1}{2} |\Im(\bar{z} z_1)| \left(\frac{1}{r_i} + \frac{1}{r} \right) (r - r_i) \\ A_4 &= \frac{1}{2} |\Im(\bar{z} z_2)| \left(\frac{1}{r} + \frac{1}{r_o} \right) (r_o - r) \end{aligned} \quad (2.7)$$

$$\begin{aligned} r_i &= |z_1| = |z_4| \\ r_o &= |z_2| = |z_3| \\ r &= |z|. \end{aligned}$$

For a particular vortex, the cell which contains it can be found by requiring to satisfy the following two conditions,

1) radial direction ;

$$r_i < |z| < r_o, \quad (2.8a)$$

2) circumferential direction ;

$$\Im(\bar{z} z_1) \Im(\bar{z} z_4) < 0, \quad (2.8b)$$

z denoting the position of the vortex as that in eqs. (2.7)

2.2.2 The velocity field

The velocity at any point within the flow field is stipulated to be estimated by bilinear interpolation of the velocities at the four corners of the cell within which the point is located. This means that the velocity field is depicted by the velocities at nodes. The velocity induced by a vortex in the flow field and its image within the cylinder is given, from eq. (2.4), by

$$\bar{w}(z) = -\frac{i\Gamma}{2\pi} \left[\frac{1}{z - z_o} - \frac{1}{z - z_i} \right] \quad (2.9)$$

Using this expression, the following two kinds of the influence coefficients are calculated :

(1) the node to node influence coefficients

$$\overline{W}_{nn}(z_{nj}; z_{nk}) = \begin{cases} \frac{i}{2\pi} \frac{1}{z_{nj} - (z_{nk})_i}, & \text{for } k = j, \\ \frac{-i}{2\pi} \left[\frac{1}{z_{nj} - z_{nk}} - \frac{1}{z_{nj} - (z_{nk})_i} \right], & \text{for } k \neq j, \end{cases} \quad (2.10)$$

(2) the node to control point influence coefficients

$$\overline{W}_{pn}(z_{pj}; z_{nk}) = \frac{-i}{2\pi} \left[\frac{1}{z_{pj} - z_{nk}} - \frac{1}{z_{pj} - (z_{nk})_i} \right] \quad (2.11)$$

$(z_{nk})_i$ denoting the inverse point of the k -th node z_{nk} . The second set of the influence coefficients is needed to expedite calculation of the velocities at the control points on the cylinder surface, which are used to determine the strengths of the nascent vortices.

The velocity occurring at the j -th node and the j -th control point on the cylinder surface at a particular time step is then given, respectively, by

$$\overline{w}(z_{nj}) = 1 - \frac{1}{z_{nj}^2} + \sum_{k=1}^N \Gamma_{nk} \overline{W}_{nn}(z_{nj}; z_{nk}) \quad (2.12)$$

$$\overline{w}(z_{pj}) = 1 - \frac{1}{z_{pj}^2} + \sum_{k=1}^N \Gamma_{nk} \overline{W}_{pn}(z_{pj}; z_{nk}) \quad (2.13)$$

where Γ_{nk} means the vortex strength at the k -th node at the time step and N denotes number of the total nodes. After the velocity at each node of the grid is calculated from the nodal vortex strength and the node to node influence coefficients by the above equation, the velocity at any point in the flow field is determined from the following expression of bilinear interpolation :

$$w = \frac{1}{A} \sum_{i=1}^4 A_i w_i \quad (2.14)$$

where w_i ; the velocity at the i -th node

A_i ; see Fig. 2

A ; area of the cell.

2.3 The nascent vortices

2.3.1 The strength

As mentioned earlier, this strength is usually determined so that the tangential velocity at the control point on the cylinder surface vanishes which results in the following simultaneous linear equations :

$$-\frac{i}{2\pi} \sum_{k=1}^m \gamma_k \left[\frac{1}{z_{pj} - \sigma_k e^{i\alpha_k}} - \frac{1}{z_{pj} - e^{i\alpha_k}/\sigma_k} \right] + \overline{w}(z_{pj}) = 0$$

Because of the oversensitive dependency of the strength γ on the distance between the cylinder surface and the radial position of the nascent vortex σ_k , this way of determining the strength is discarded in the present study. Instead, the strength is directly determined from the tangential velocity at the control point which is taken as the point where the radial line to the nascent vortex intersects the cylinder surface. Thus the strength is determined from :

$$\gamma_j = -\Im[\overline{w}(z_{pj})z_{pj}] \Delta\theta, \quad j = 1, 2, \dots, m \quad (2.15)$$

The vortex strength determined in this way is not independent of the distance between the cylinder surface and the position of the nascent vortex but less sensitive to it than in the other way. In addition, it has logical advantage that the strength density determined by the flow field itself is used to calculate the vortex strength.

2.3.2 The position

If the nascent vortices are put on the cylinder surface where the sheet vortex is supposed to locate, the vortex shedding does not occur because of zero normal velocity there. This demands the initial starting point of a nascent vortex to be a small distance off the cylinder surface. The radial position of a nascent vortex is then expressed by

$$\sigma_k = 1 + \delta \quad k = 1, 2, \dots, m \quad (2.16a)$$

The suitable value for δ is sought through the numerical experiments.

As many nascent vortices as the radial lines of the grid are to be introduced every time step, each one being put at midpoint between the two neighbouring radial lines. That is, the circumferential position of the k -th nascent vortex is specified by

$$\alpha_k = (k - 0.5) \Delta \theta \quad k = 1, 2, \dots, m \quad (2.16b)$$

2.4 Convection of the vortices

The nascent vortices determined in the above section are merged sequentially to the vortices shed already into the flow field as the following equations show :

$$\Gamma_{M_t+k} = \gamma_k \quad (2.17)$$

$$z_{M_t+k} = \sigma_k e^{i\alpha_k} \quad k = 1, 2, \dots, m \quad (2.18)$$

The total number of the shed vortices should also be adjusted as

$$(M_t)_{new} = M_t + m \quad (2.19)$$

After calculating the velocities at all nodes by eq.(2.12), the velocity at the position of a particular vortex is evaluated from these results as the eq.(2.14) shows. Search of the relevant cell can be accomplished again by requiring to satisfy the conditions shown in eq.(2.8). The convection velocity being available, the new position of the

vortex for the next time step can be readily predicted by some time marching scheme. Simple forward difference scheme is used in the present study as follows :

$$z_{k,new} = z_{k,old} + w(z_{k,old}) \Delta t \quad (2.20)$$

2.5 Stimulation of the asymmetry

Although a cylinder has perfect geometrical symmetry with respect to the flow direction and the consequent symmetric influence coefficients, the asymmetry of vortex shedding in the DVM analysis of flow does eventually occur due to the round-off error of calculation even without the aid of any compulsory asymmetry-inducing scheme. However, this process is too time-consuming and, more significantly, no realistic vortex distribution pattern is produced in that way. Hence, a positive means of stimulating asymmetry had better be introduced at the early stage of vortex shedding. Disturbance of vortex distribution by adding extra displacements to the vortices shed from one side of the cylinder is frequently used as such a means and employed in the present investigation. The suitable magnitude of the displacement and duration of imposing the disturbance still remain to be decided through numerical experiments. What is basically required to evolve a realistic stabilized vortex distribution pattern is that these factors should be in good harmony with the properties of the group of vortices first shed from the other side of the cylinder.

Gradual introduction of disturbance over a number of time steps is chosen in this study. Specifically, all the vortices lying in the fourth quadrant are shifted a certain distance in the direction of the free stream for certain number of the initial time steps as the following equation shows :

$$z_{k,shifted} = z_k + \xi \quad (2.21)$$

ζ denoting the displacement per time step.

2.6 The force calculation

The force components exerted to the cylinder by the fluid due the vortex shedding are frequently calculated through the following set of formulae derived originally, but with some slight differences, by Sarpkaya[6]

$$C_D = - \sum_{k=1}^{M_t} \Gamma_k (v_k - v_{ik}) \quad (2.22a)$$

$$C_L = \sum_{k=1}^{M_t} \Gamma_k (u_k - u_{ik}) \quad (2.22b)$$

These formulae were derived from the extended Blasius theorem under the assumption that no additional vortices other than those already shed into the flow field appear during the small interval of time of the time derivation. The time step of introduction of the nascent vortices being arbitrary, this assumption seems not logical enough because a set of the nascent vortices should be there however weak their strength change in the time interval may be. From this point of view, Lee[7] derived another set of formulae which have additional terms coming into existence through the nascent vortices grown during the time interval, in the form of the growth rate, as shown below :

$$C_D = - \sum_{k=1}^{M_t} \Gamma_k (v_k - v_{ik}) - \sum_{k=1}^m \frac{d\gamma_k}{dt} \left(1 - \frac{1}{\sigma_k}\right) \sin \alpha_k \quad (2.23a)$$

$$C_L = \sum_{k=1}^{M_t} \Gamma_k (u_k - u_{ik}) + \sum_{k=1}^m \frac{d\gamma_k}{dt} \left(1 - \frac{1}{\sigma_k}\right) \cos \alpha_k \quad (2.23b)$$

The force coefficients are calculated with these two sets of formulae to see the difference they bring in.

2.7 The growth rate of the nascent vortices

As the strengths of the nascent vortices are calculated from eq.(2.15), the growth rates are expressed as the time derivative of this equation,

$$\frac{d\gamma_j}{dt} = -\Im \left[\frac{d\bar{w}(z_{pj})}{dt} z_{pj} \Delta\theta \right] \quad (2.24)$$

The rate of change of the conjugate complex velocity at the control point on the cylinder surface in the above expression should be evaluated from the rate of change of the vortex strength at each node of the grid which is in turn dependent on the rate of change of area element due to the motion of each vortex in a cell. Although this process is logically in conformity with the vortex-in-cell method, it contains much more complicated computational works compared with the process of direct calculation from the motion of vortices. If the velocity occurring at the control points on the cylinder surface is to be calculated directly from the vortices existing in the flow field, the relevant expression is, instead of eq. (2.13),

$$\bar{w}(z_{pj}) = 1 - \frac{1}{z_{pj}^2} - \frac{i}{2\pi} \sum_{k=1}^{M_t} \Gamma_k \left[\frac{1}{z_{pj} - z_k} - \frac{1}{z_{pj} - (z_k)_i} \right] \quad (2.25)$$

and therefore the time derivative of this velocity is expressed as

$$\frac{d\bar{w}(z_{pj})}{dt} = -\frac{i}{2\pi} \sum_{k=1}^{M_t} \Gamma_k \left[\frac{w_k}{(z_{pj} - z_k)^2} - \frac{w_{ik}}{(z_{pj} - (z_k)_i)^2} \right] \quad (2.26)$$

where

- w_k : the complex velocity of the k-th vortex
- w_{ik} : the complex velocity of the image of the k-th vortex

2.8 Summary of the computational procedure

The computational procedure of the present investigation based on the DVM analysis is summarized as follows :

- 1) read in the computational parameters,
- 2) generate the grid system,
- 3) fix the position of the nascent vortices,
- 4) calculate the influence coefficients,
- 5) calculate the redistribution ratios for the nascent vortices,
- 6) distribute the vortex strength, if any, to the nodes, eq.(2.6),
- 7) calculate the velocity occurring at the control points on the cylinder surface,
- 8) calculate strengths of the nascent vortices,
- 9) distribute these strengths to the nodes,
- 10) join these vortices to the sequence of the vortices shed already,
- 11) calculate velocity induced at each node of the grid,
- 12) calculate the convection velocity of each vortex,
- 13) calculate the force coefficients C_L , C_D ,
- 14) predict the new positions of the vortices,
- 15) apply disturbance for asymmetry(initial time steps only),
- 16) write out current positions of the vortices and values of C_L and C_D ,
- 17) repeat the procedure again from the step 6).

3. Selection of the computational parameters

The parameters which should be set before the computation begins are :

- 1) number of the nascent vortices m ,
- 2) the distance between the nascent vortices and the cylinder surface δ ,
- 3) magnitude of the time step Δt ,
- 4) disturbance to induce asymmetry.

1) number of the nascent vortices

This number determines degree of resolution of the flow field. For greater value of this number therefore, smaller value of time step is to be used

to maintain the same scale to deal with distance. It is somewhat surprising from this point of view to notice that in the past attention and effort were largely concentrated to find the most suitable value of the time step independently of other parameters. Because of the convection mechanism in the DVM, the suitable value of δ of eq.(2.16a) also seems to have some connection with this number as will be discussed in the following.

The restriction on this number comes from two different aspects concerned with the problem: the first is the practical side of the job, that is, computational load as it builds up quickly as the number increases and the second is that it is not rational to try to improve the degree of resolution alone when there is more fundamental source of error originating from the inviscid fluid modelling. This consideration made some number between fifty and one hundred appear to be reasonable and sixty were chosen for m in the present investigation.

2) Position of the nascent vortices

It is natural to put a nascent vortex circumferentially at midpoint between two neighbouring radial lines of the grid, as eq.(2.16b) shows. But the choice of the radial position is not so obvious. The thickness of the boundary layer appears to offer a good standard for determination of this position with respect to the cylinder surface and deserves serious consideration because some device that can be incorporated to the method to account for the Reynolds number dependency of a flow might be found from this strategy. If the gap between the nascent vortices and the cylinder surface denoted by δ in eq.(2.16a) is determined from this idea, it can be too small when the Reynolds number is very high for the nascent vortices to convect, apart from the difficulty of calculating the unsteady boundary layer thickness and overcoming the embarrassed situation to determine the boundary layer thickness after the separation points. The experience suggested that smaller mesh size, and hence more

nascent vortices, was needed for smaller value of δ to help the vortices to convect. This means that the smaller mesh size is needed for higher Reynolds number flow, as in other numerical methods, if δ is to be determined based on the boundary layer thickness.

In spite of the above possibility of development, the DVM at the present stage claims to be a technique of simulating flow of infinite Reynolds number because of inviscid flow modeling. The effect of viscosity being out of consideration, the present study remains within this traditional attitude. With the number of nascent vortices fixed as sixty, the suitable value for δ has been therefore sought through numerical experiments and found to be 0.1.

3) Time step

This is one of the parameters which have been the subjects of intensive investigation through the history of development of the DVM. Yet no general principle has been established for the choice of good working value on a rational basis. Instead, the vortex distribution generated with a value of the time step served as the standard to judge adequacy of the chosen value. Historically, values⁽¹⁰⁾⁽¹¹⁾ between 0.008–0.32 have been used in various context of the DVM. Downie⁽¹²⁾ et al. used 0.2 determined from

$$\delta/\Delta t = 0.5$$

for a prescribed value of $\delta = 0.1$ and obtained a good vortex distribution pattern. This is an example of interrelating the time step with other parameter.

Since the parameters have interrelationship between them and are dependent on the method of introducing the nascent vortices, the principle to find the suitable value of the time step may have to be sought within the particular context of the DVM followed by the individual study. When a grid system is used to discretize the flow field, as

is in the present study, it seems natural to require for this value to keep the same degree of resolution of the flow field specified by the mesh size. Since the representative mesh size is $a \Delta\theta$ and the typical displacement of a vortex per time step is $U \Delta t/2$ both in terms of dimensional variables, the appropriate nondimensional time step may be found as

$$\begin{aligned} \Delta t &= 2 \Delta\theta \\ &= 4\pi/m \end{aligned}$$

As m is set as 60, this value becomes about 0.2 which is chosen for the time step in the present study.

4) disturbance to induce asymmetry

The first ten time steps are chosen for the duration of imposing the disturbance from the consideration that they will be much smaller than the number of time steps involved in one period of vortex shedding and yet long enough to avoid the shock that the flow field may undergo if the disturbance be concentrated to a single time step. Under this premise, the suitable value of ξ of eq. (2.21) has been sought through numerical experiments and 0.04 has turned up to produce the best evolution of vortex distribution pattern in the present study.

4. The computed results

4.1 the vortex distribution pattern

With $m = 60$ and $\Delta t = 0.2$ both fixed, much amount of numerical experiments was performed for a systematic variation of the values of δ and ξ . The vortex distribution at time step 300 obtained with $\delta = 0.1$ and $\xi = 0.04$ is shown in Fig.3. For this particular set of parameters, the vortex distribution pattern was found to maintain stability for the longest period. When δ is changed to 0.06 and 0.08 with ξ fixed at 0.04, the vortex distribution patterns at the time step 200



Fig. 3 The vortex distribution pattern at $t = 60$ with the parameters, $\delta = 0.1, \Delta t = 0.2, \xi = 0.04$



Fig. 4 The vortex distribution pattern at $t = 40$ with the parameters, $\delta = 0.06, \Delta t = 0.2, \xi = 0.04$

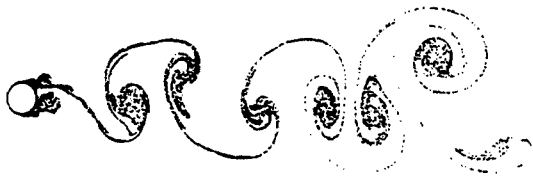


Fig. 5 The vortex distribution pattern at $t = 40$ with the parameters, $\delta = 0.08, \Delta t = 0.2, \xi = 0.04$



Fig. 6 The vortex distribution pattern at $t = 40$ with the parameters, $\delta = 0.1, \Delta t = 0.2, \xi = 0.03$



Fig. 7 The vortex distribution pattern at $t = 60$ with the parameters, $\delta = 0.1, \Delta t = 0.2, \xi = 0.05$

are shown in Fig.4 and Fig.5 respectively for comparison. Slightly better patterns may well be produced in both cases with finely adjusted ξ but no great improvement is expected. Moreover unreasonable scattering of C_D and C_L values calculated with these sets of parameters made it convincing that δ smaller than 0.1 offered no prospect unless the mesh size was reduced. Thus 0.1 is selected as the value for δ and the best working ξ was sought for and found to be 0.04. Fig.6 and Fig.7 show the vortex distribution patterns when 0.03 and 0.05 respectively are used for ξ , these patterns being in contrast to that of Fig.3. The reason that the vortex distribution pattern obtained with $\xi = 0.04$ exhibits such stability up to far greater number of time steps than that with any other ξ is supposed to be that amount of disturbance happens to be exactly what is needed to be in balance with the requirement of the cluster of vortices to be shed from the other side of the cylinder.

4.2 the force coefficients

Fig.8 shows the drag coefficients and the lift coefficients calculated with the same set of the

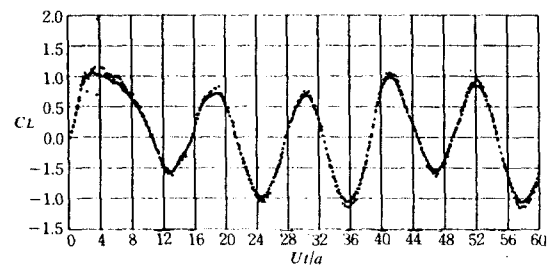
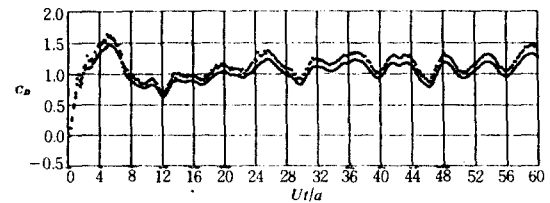


Fig. 8 C_D and C_L curve,

- : Lee's force formulae
- : Sarpkaya's force formulae

parameters as those used to obtain Fig.3. Values computed by Lee's formulae and by Sarpkaya's ones are plotted together. The term containing growth rate of the nascent vortices contributes about ten extra percent to the final values in both the drag coefficients and the lift coefficients, making the results of Lee's formulae that much greater than those of Sarpkaya's. The predicted drag coefficients are almost directly comparable with the measured values (Fig.9[13]). Even the sharp increase of C_D up to about 1.6 just after the impulsive start is the same. Except the initial peak, the measured value of C_D , mildly oscillating, lies between 1.0 and 1.3 depending on the Reynolds number for the presented time range of 0 to 24. The predicted C_D seems to be slightly smaller than the measured for the corresponding time interval but as it becomes greater immediately after this interval no conclusive comparison can be made. However, a fairly cer-

tain discrepancy may be that the predicted values show more distinct undulation than the measured ones. This favourable comparison as for the drag unfortunately does not signify that the present method is a reliable working tool as for the lift as well. The predicted C_L values are about twice as large as the measured ones shown in Fig.10[13]. That the DVM excessively overestimates lift is inevitably followed in the present treatment, the trend being generally accepted as a part of intrinsic attribute of the DVM. To have comparable lift coefficients, an ad-hoc contrivance or ammendment of modelling to reflect the effect of viscosity is to be invoked. Nonetheless a numerical procedure which faithfully and reliably works for the DVM without such additional measures is of prerequisite necessity before any improvements of the method are attempted for more realistic predictions. The period of lift fluctuation compares much more

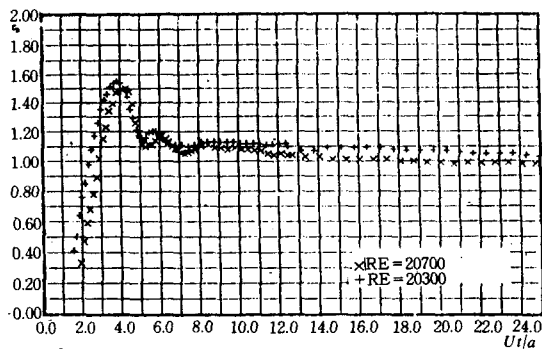


Fig. 9a C_D vs Ut/a for Reynolds numbers 20300 and 20700

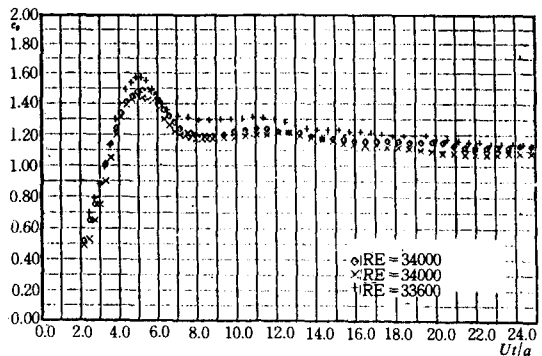


Fig. 9b C_D vs Ut/a for Reynolds numbers 33600 and 34000

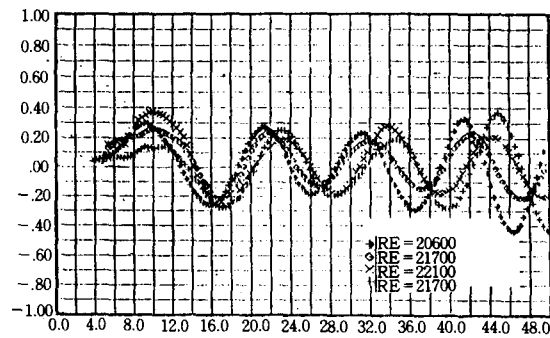


Fig. 10a C_L vs Ut/a for Reynolds numbers 20600, 22100, and 21700

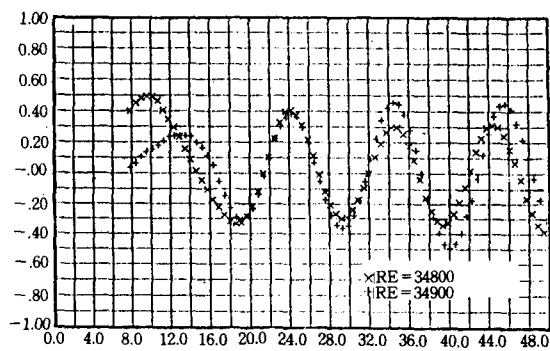


Fig. 10b C_L vs Ut/a for Reynolds numbers 34800 and 34900

favourably with that of the measured lifts, suggesting that viscosity plays a negligible role in determining the period of alternation of vortex shedding.

5. Conclusions

The vortex shedding from a circular cylinder can be quite realistically simulated by the DVM when the computation parameters are suitably chosen. The parameters are interrelated and the number of nascent vortices is the fundamental factor from which the other parameters can be deduced to maintain the same degree of approximation. The drag can be estimated to a reliable level of accuracy without any provision about the role of the viscosity but the situation is different with the lift. The lift fluctuation looks, however, hardly influenced by the viscosity. Some minor but specific points may be summarized as follows :

1) it is a good policy to determine the strength of the nascent vortices from the tangential velocity at the cylinder surface rather than to determine them so that the tangential velocities vanish,

2) the number of the nascent vortices can be freely chosen but once it is fixed the other parameters are to be in conformity with this number,

3) a working rule to determine the reasonable gap between the nascent vortices and the cylinder surface is to keep it the same as the distance between two adjacent nascent vortices,

4) the reasonable time interval of introduction of the nascent vortices may be determined from $\Delta t = 4\pi / m$,

5) the asymmetry can be stimulated with good results by gradual imposition of disturbance spread over a small number of the initial time steps,

6) the drag is reliably estimated by the present procedure but some further implementation is needed to predict the lift by the matching pre-

cision.

References

- [1] Gerrard, J.H., *Numerical Computation of the magnitude and Frequency of the Lift on a Circular Cylinder*, Phil. Trans. of the Royal Soc. of London, Series A, vol. 261, pp. 137-162, 1966-7
- [2] Clements, R.R., *An inviscid model of two-dimensional vortex shedding*, J. Fluid Mech., vol. 57, part 2, pp. 321-336, 1973
- [3] Sarpkaya, T. and Shoaff, R.L., *A discrete-vortex analysis of flow about stationary and transversely oscillating circular cylinders*, Naval Postgraduate School Technical Report no : NPS-69SL79011, 1979
- [4] Fink, P.T. and Soh, W.K., *Calculation of vortex sheets in unsteady flow and applications in ship hydrodynamics*, Proc. 10th symp. Naval Hydro., MIT Cambridge, pp. 463-491. 1974
- [5] Lewis, R.I. and Porthouse, D.T.C., *Recent Advances in the Theoretical Simulation of Real Fluid Flows*, Trans. NECIES, vol. 99, pp. 88-104, 1983
- [6] Sarpkaya, T., *Lift, Drag, and Added-Mass Coefficients for a Circular Cylinder Immersed in a Time Dependent Flow*, J. of Appl. Mech., Trans. ASME, pp. 13-15, 1963
- [7] Lee, D.K., *Formulas for the Calculation of Lift and Drag Exerted to a Curcular Cylinder due to the Flow Acceleration and the Vortex Shedding Simulated by Discrete Vortices*, J. of Engineering Research, Univ. of Ulsan, vol. 22, no. 2, 1992
- [8] Milne-Thomson, L.M., *Theoretical Hydrodynamics*, 5th ed., Macmillan 1968
- [9] Christiansen, J.P., *Numerical Simulation of Hydrodynamics by the Method of Point Vortices*, J. of Comp. Physics, vol. 13, pp. 363-379. 1973
- [10] Aarsnes, J.V., Faltinsen, O. and Pettersen, B., *Application of a vortex tracking method to current forces on ships*, Proc. IAHR Symp. on Separated Flow Around Marine Structures,

- Trondheim, pp. 309-346, 1985
- [11] Kiya, M. and Arie, M., *A contribution to an inviscid vortex-shedding model for an inclined flat plate in uniform flow*, J. Fluid Mech., vol. 82, part 2, pp. 223-240, 1977
- [12] Downie, M. J., Murray, B.A. and Bettess, P., *Calculation of the force coefficients of a tubular jacket structural member with an appurtenance by the discrete vortex method*, Int. J. for Num. Meth. in Engineering, vol. 27, pp. 153-167, 1989
- [13] Sarpkaya, T., *Impulsive flow about a circular cylinder*, Naval Postgraduate School Report : NPS-69SL-78-008, 1978